

Document downloaded from:

<http://hdl.handle.net/10251/179427>

This paper must be cited as:

Montilla, F.; Quintero-Jaime, AF.; Huerta, F.; Quijada, C. (2021). Determination of exciton diffusion coefficient in conjugated polymer films: Novel methods based on spectroelectrochemical techniques. *Electrochimica Acta*. 387:1-6.
<https://doi.org/10.1016/j.electacta.2021.138419>



The final publication is available at

<https://doi.org/10.1016/j.electacta.2021.138419>

Copyright Elsevier

Additional Information

Electrochimica Acta

Determination of Exciton Diffusion Coefficient in Conjugated Polymer Films: Novel Method based on Spectroelectrochemical Techniques --Manuscript Draft--

Manuscript Number:	ISE_2020_ELECTACTA-S-20-07742R1
Article Type:	VSI:ISE-2020
Keywords:	Conjugated Polymers; , MEH-PPV; electrofluorochromism; electrochemical band gap; exciton dynamics; polaron-exciton annihilation; polaron cross-section
Corresponding Author:	Francisco Montilla Universidad de Alicante Alicante, Spain Spain
First Author:	Francisco Montilla
Order of Authors:	Francisco Montilla Andrés F. Quintero-Jaime Francisco Huerta César Quijada
Manuscript Region of Origin:	SPAIN
Abstract:	<p>The understanding of exciton dynamics is a central issue in the operation of conjugated polymer-based optoelectronic devices, like solar cells, light-emitting diodes or electrochemiluminescent cells. In this work, we explore the applicability of combined in situ electrochemical fluorescence and UV-vis spectroscopies for the study of electrochemically induced quenching of photoluminescence as novel tools for the determination of exciton diffusion in a model conjugated polymer, poly[2-methoxy-5-(2-ethylhexyloxy)-1,4-phenylvinylene] (MEH-PPV). It is demonstrated that the quenching process observed upon electrochemical doping follows a linear Stern-Volmer mechanism at low doping levels, with a time-independent rate constant typical of diffusion-controlled annihilation processes. From the Stern-Volmer rate constant and the exciton-polaron critical distance, an exciton diffusion coefficient is derived whose value is in close agreement with those reported in the literature. These results support the suitability of these spectroelectrochemical techniques as fast and powerful alternative tools for the reliable determination of exciton diffusion coefficients in conjugated polymers.</p>

1
2
3
4
5
6
7
8
9
10
11
12
13
14
15
16
17
18
19
20
21
22
23
24
25
26
27
28
29
30
31
32
33
34
35
36
37
38
39
40
41
42
43
44
45
46
47
48
49
50
51
52
53
54
55
56
57
58
59
60
61
62
63
64
65

Determination of Exciton Diffusion Coefficient in Conjugated Polymer Films: Novel Method based on Spectroelectrochemical Techniques

Francisco Montilla¹, Andrés F. Quintero-Jaime¹, Francisco Huerta², César Quijada²

¹ Departamento de Química Física e Instituto Universitario de Materiales de Alicante. Universidad de Alicante. Apdo. de Correos 99, E-03080 Alicante, Spain

² Departamento de Ingeniería Textil y Papelera, Universitat Politècnica de València, Plaza Ferrandiz y Carbonell, 1, E-03801 Alcoy, Spain.

francisco.montilla@ua.es

1
2
3
4 **Abstract**
5

6 The understanding of exciton dynamics is a central issue in the operation of conjugated
7 polymer-based optoelectronic devices, like solar cells, light-emitting diodes or
8 electrochemiluminescent cells. In this work, we explore the applicability of combined *in situ*
9 electrochemical fluorescence and UV-vis spectroscopies for the study of electrochemically
10 induced quenching of photoluminescence as novel tools for the determination of exciton
11 diffusion in a model conjugated polymer, poly[2-methoxy-5-(2-ethylhexyloxy)-1,4-
12 phenylvinylene] (MEH-PPV). It is demonstrated that the quenching process observed upon
13 electrochemical doping follows a linear Stern-Volmer mechanism at low doping levels, with
14 a time-independent rate constant typical of diffusion-controlled annihilation processes. From
15 the Stern-Volmer rate constant and the exciton-polaron critical distance, an exciton diffusion
16 coefficient is derived whose value is in close agreement with those reported in the literature.
17
18 These results support the suitability of these spectroelectrochemical techniques as fast and
19 powerful alternative tools for the reliable determination of exciton diffusion coefficients in
20 conjugated polymers.
21
22
23
24
25
26
27
28
29
30
31
32
33
34
35
36
37
38
39
40
41
42
43
44
45
46
47
48
49
50
51
52
53
54
55
56
57
58
59
60
61
62
63
64
65

1. Introduction

Exciton dynamics play a central role in the operation of most organic optoelectronic devices. These processes are critical in working OLEDs, organic photovoltaic cells or luminescent electrochemical cells [1,2]. For example, in organic photovoltaic cells, the photogenerated excitons must move to interfacial zones to be dissociated into charge carriers and, consequently, large exciton diffusion lengths are required to enhance efficiency. A major part of these devices is based on conjugated polymers since they are attractive for the high amount of processing techniques that allow their use as thin films in flexible and lightweight substrates.

The process of exciton diffusion in polymer films can be characterized either by spectroscopic techniques, which measure the efficiency of radiated photons in the presence of quenchers or by charge carrier techniques, which measure photogenerated charges resulting from quenched excitons [3]. Among the spectroscopic techniques, those based on the quenching of photoluminescence are widely extended. The photoluminescence (PL) of thin films is measured in the absence and in the presence of a quenching site and the exciton diffusion length is derived from the PL quotient. In these studies, a statistically significant number of experiments are required to obtain consistent results and therefore many samples must be prepared. Typical quenchers include electron acceptors as fullerene-C₆₀, subphthalocyanines or molecular dyes, prepared as interfacial films or blended with the polymer in bulk heterojunction architectures [4–6].

The electronic structure of conjugated polymers can be modified through a reversible electrochemical charge injection, which leads to the formation of charged states, such as polarons, polaronic bands or bipolarons, among others [7]. By coupling an electrochemical excitation system to a suitable spectroscopic technique, the spectral features of those excited

1
2
3
4 states can be characterized. In particular, electrochemical *in situ* UV-vis spectroscopy has
5
6 been used to obtain the energy of the intragap transition in doped conjugated polymers and
7
8 to quantify polaron absorption cross-sections, which are key parameters used for the
9
10 development of electrically pumped lasers and for the optimization of organic light-emitting
11
12 diodes, among other applications [8,9]
13

14
15
16 A related spectroelectrochemical technique, the electrochemical *in situ* fluorescence
17
18 spectroscopy (also known as electrofluorochromism [10]) is a relatively novel tool that has
19
20 been applied to the characterization of luminescent molecular systems and to the
21
22 development of novel optoelectronic devices [11–15]. The use of electrochemical
23
24 instrumentation allows fine and precise control of the quencher concentration permitting
25
26 simultaneous analysis of exciton dynamics within a single sample of the conjugated polymer
27
28 [16–18].
29
30

31
32
33 In the present work, a combination of electrochemical *in situ* steady-state fluorescence
34
35 spectroscopy and UV-vis spectroscopy has been employed for the first time to determine the
36
37 diffusion coefficient of excitons. The material selected for this study is the orange-red emitter
38
39 MEH-PPV. Among the family of conjugated PPV polymers, it constitutes an archetypical
40
41 material showing a huge variety of optoelectronic applications [19,20].
42
43
44
45
46

47 **2. Experimental section**

48 *2.1. Materials*

49
50
51 MEH-PPV was purchased from Sigma-Aldrich (average Mn 150000-250000). Fluorine-
52
53 doped tin oxide (FTO)-coated glass substrates (FTO-AGC 80, 70–90 Ω) employed as
54
55 electrode support in all the *in situ* spectroelectrochemical experiments was provided by
56
57 SOLEMS. Anhydrous tetrahydrofuran (THF, $\geq 99.9\%$), anhydrous acetonitrile (ACN,
58
59
60
61

1
2
3
4 $\geq 99.8\%$), tetrabutylammonium tetrafluoroborate (TBATFB $\geq 99\%$) and ferrocinium
5
6 hexafluorophosphate (Fc, $\geq 97\%$) were supplied by Sigma-Aldrich.
7
8
9

10 11 12 13 *2.2. In situ spectroelectrochemical characterization*

14
15
16 *In situ* spectroelectrochemical measurements (absorption, steady-state PL), were
17
18 performed in a modified, 1 cm length, fused silica cell capped with a Teflon plate, which also
19
20 served as the electrode support [21]. Working electrode was prepared with FTO modified
21
22 with a polymer film of MEH-PPV. Prior to the polymer deposition, FTO electrodes were
23
24 cleaned by sonication in an acetone bath. Afterwards, 20 μL of MEH-PPV previously
25
26 dissolved in THF (2.0 mg mL^{-1}) were drop-casted over 1cm^2 of the FTO substrate. This
27
28 working electrode was immersed in a solution of 0.1 M TBATFB in ACN. The counter
29
30 electrode was a platinum wire and a silver wire was used as the pseudoreference electrode,
31
32 both immersed in the same solution and protected by a glass capillary tube. The reference
33
34 electrode was calibrated using the ferricenium/ferrocene redox couple (Fc/Fc⁺). Air was
35
36 purged from the electrochemical cell by bubbling with an argon flow for 10 min and the inert
37
38 atmosphere was maintained during all the experiments.
39
40
41
42
43
44

45
46 Electrochemical experiments were carried out by using a function generator (EG&G Parc
47
48 model 175) connected to a potentiostat-galvanostat (Pine Instrument model AFCBP1).
49
50 Photoluminescence (PL) and UV-vis spectra were acquired using a PTI QuantaMaster
51
52 spectrofluorometer (model QM-62003SE) and an Ocean Optics spectrophotometer (Flame
53
54 model Avantes DH-2000-S and optical fibers Ocean Optics QP100-2-UV/VIS GF052107-
55
56 101), respectively. The density of the polymer was determined by helium
57
58
59
60
61
62
63
64
65

1
2
3
4 microultraviolet (QUANTACHROME INSTRUMENTS) obtaining a value of 1.176 g
5
6 cm^{-3} for the solid polymer. Resulting electrochemically-induced absorption (ECIA) UV-vis
7
8 spectra for MEH-PPV films were obtained as follows. A first single reference spectrum was
9
10 acquired at the E_{onset} , representing the electronic state of the neutral (undoped) film. Then,
11
12 sample spectra were collected at increasing applied potentials, E_{app} , representing the
13
14 electronic state of the polymer at different oxidation states during the *p*-doping process.
15
16 Finally, the unique reference spectrum was subtracted from each sample spectra and the
17
18 resulting absorbance change, ΔA , is plotted against wavelength. *In situ* fluorescence
19
20 measurements were performed in a modified fluorescence cell (1 cm length quartz cell).
21
22 Details on the cell design have been shown in a previous article [21].
23
24
25
26
27
28
29
30
31

32 **3. Results and discussion**

33 *3.1. Optical and electrochemical characterization*

34
35 Fig. 1.a shows the absorption (black curve) and the PL emission (red curve) spectra of
36
37 a MEH-PPV polymer deposited as a thin film onto an FTO electrode. The absorption
38
39 maximum at 505 nm corresponds to the $\pi\pi^*$ transition of conjugated chains, whereas the
40
41 fluorescent emission displays a maximum at 594 nm and a well-defined vibronic feature at
42
43 around 637 nm.
44
45
46
47
48
49
50
51
52
53
54
55
56
57
58
59
60
61
62
63
64
65

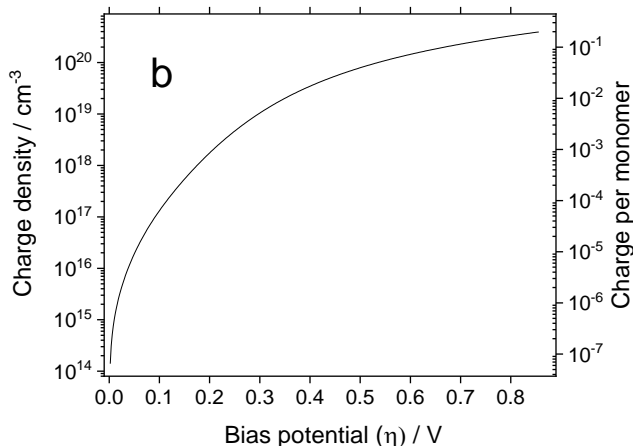
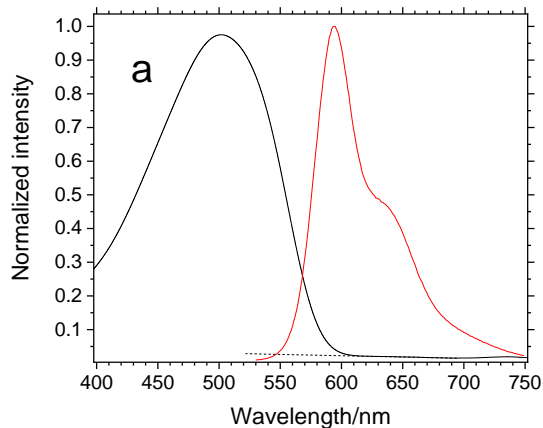


Figure 1: Absorption and emission spectra ($\lambda_{\text{exc}}=500$ nm) of MEH-PPV films on FTO electrodes. b) Injected charge as a function of the bias potential applied over the onset of the *p*-doping process.

Since MEH-PPV is an electroactive material, it undergoes reversible doping by electrochemical methods. Fig. S1 in the supporting information shows the cyclic voltammogram of MEH-PPV including the reversible *p*- and *n*-doping processes in the polymer. Formation of positive polaronic species (*p*-doping) along the polymer chains starts

1
2
3
4 at around $E_{\text{onset}} = -0.6$ V, derived from the onset potential of the oxidation current recorded
5
6 during the forward sweep. In the reverse scan, a reduction feature peaking at around -0.7 V
7
8 appears in the CV, which corresponds to the dedoping of oxidized MEH-PPV. The
9
10 electrochemical processes associated to n -doping of the polymer are observed in the left
11
12 branch of the voltammetric curve. In the scan to negative potentials, n -doping starts at a
13
14 reduction onset potential of -2.6 V, while reversible dedoping occurs with an oxidation
15
16 peaking at around -2.6 V, after scan reversal. Since the oxidation onset for p -doping and the
17
18 reduction onset of the n -doping corresponds to the energy of HOMO and LUMO levels of
19
20 conjugated chains, respectively, the so-called electrochemical bandgap can be obtained easily
21
22 from CV curves [22,23]. In the present case, the HOMO-LUMO difference calculated from
23
24 the experiment in Fig. S1 amounts to 1.97 eV, in close agreement with those 2.00 eV
25
26 measured for the optical bandgap obtained from the onset of the red-edge $\pi\pi^*$ absorption
27
28 band.
29
30
31
32
33
34

35
36 Fig 1.b shows the concentration of charges electrochemically injected within the film
37
38 (i.e. the charge density) and the resulting number of charges per monomer unit against the
39
40 bias potential. The presented bias potential, η , refers to the difference between the applied
41
42 potential at each point and the onset potential for p -doping, $\eta = (E_{\text{app}} - E_{\text{onset}})$.
43
44
45
46
47

48 3.2. Spectroelectrochemical characterization of exciton diffusion

49

50
51 Electrochemically-induced absorption (ECIA) UV-vis spectroscopy is an experimental
52
53 tool that provides valuable information on optoelectronic alterations triggered by the applied
54
55 potential. The resulting ECIA-UV-vis spectra for MEH-PPV films are shown in Fig. 2.a.
56
57
58
59
60
61
62
63
64
65

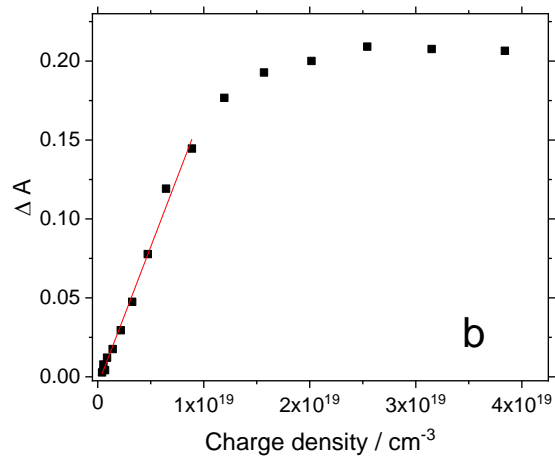
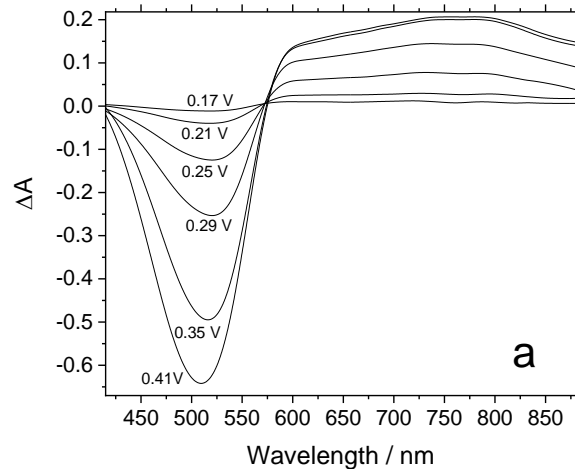


Figure 2. a) Electrochemically induced UV-vis spectra obtained during the *p*-doping process of MEH-PPV (bias potential is indicated close to each curve). b) Absorbance change of the electrochemically-induced UV-vis polaron transition band at increasing levels of *p*-doping.

1
2
3
4 As the bias potential increases, a negative absorption band appears at 517 nm
5
6 corresponding to the bleaching of $\pi\pi^*$ transition. Concurrently, a wide positive absorption
7
8 band develops at around 760 nm at increasing doping levels. The energy of the feature is
9
10 compatible with an electron hop between the HOMO level and higher subgap states of
11
12 polarons in MEH-PPV [24,25]. Fig. 2.b shows the change in the polaron peak intensity
13
14 against the injected charge. At low doping levels the intensity of the transition increases
15
16 almost linearly up to $1 \times 10^{19} \text{ cm}^{-3}$ ($\eta=0.30 \text{ V}$), thus providing a method to determine the
17
18 polaron absorption cross-section, σ , by means of Eq. 1 [8].
19
20
21
22
23

$$\sigma = \frac{2.30}{l} \frac{\Delta A}{\Delta CD} \quad (1)$$

24
25
26
27
28
29
30
31 where ΔA is the electrochemically induced absorbance change, CD is the concentration of
32
33 charge injected within the film and l is the film thickness. An absorption cross-section of
34
35 $1.18 \times 10^{-15} \text{ cm}^2$ is obtained, in agreement with literature data [26,27]. The saturation of the
36
37 polaron band occurs from a charge density close to $2 \times 10^{19} \text{ cm}^{-3}$, which corresponds to 0.01
38
39 charges per monomer unit.
40
41
42
43

44 Fig. 3.a shows *in situ* PL spectra recorded from MEH-PPV at increasing potentials
45
46 during the *p*-doping process. The black curve (bias potential $\eta= 0.0 \text{ V}$) represents the PL
47
48 emission of the polymer in the undoped state. The application of potentials beyond the doping
49
50 onset results in a progressive quenching of the emission. The complete quenching is
51
52 accomplished from a bias potential of 0.32 V (1.4×10^{19} charges cm^{-3}), a similar value
53
54 observed for the polaron band saturation in UV spectra. The initial fluorescence can be
55
56
57
58
59
60
61
62
63
64
65

recovered after applying a potential below the oxidation onset, where the polymer recovers its semiconducting state.

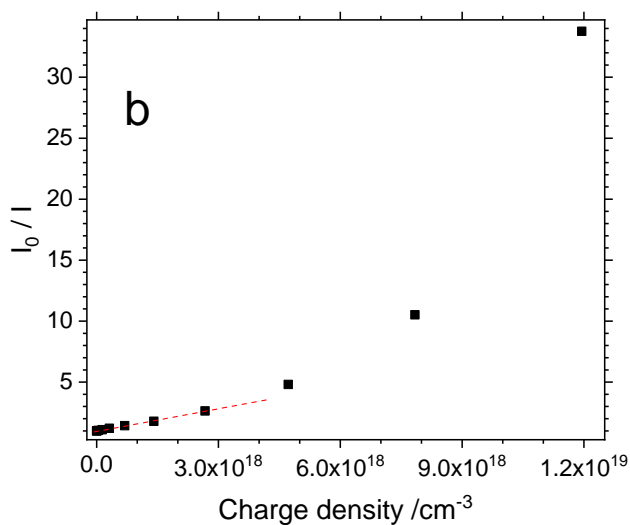
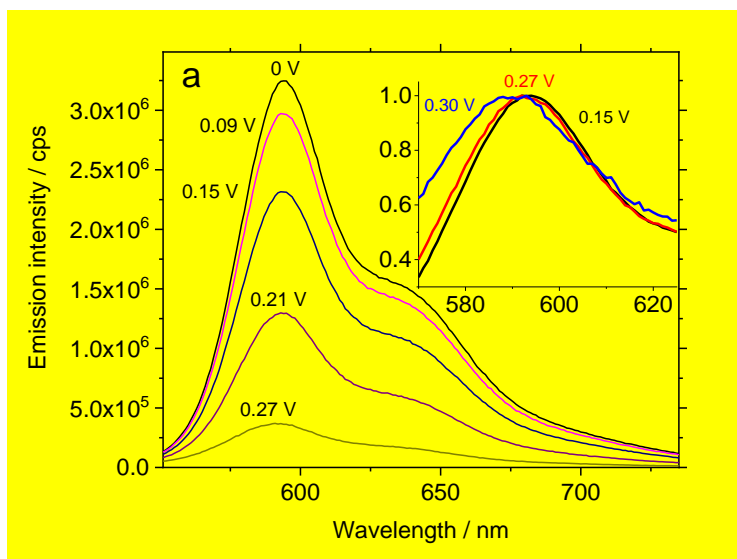
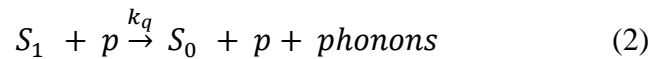


Figure 3. a) Evolution of the PL emission spectrum during the *p*-doping. Inset: Evolution of the normalized PL emission spectrum during the *p*-doping. The value of bias potential, η , is indicated close to the corresponding curve. ($\lambda_{\text{exc}} = 500 \text{ nm}$). b) Electrochemical Stern-Volmer plot for the *p*-doping process of MEH-PPV.

1
2
3
4
5
6
7 The evolution of the shape of the PL spectrum can be appreciated in the inset to Fig.
8
9 3.a, where normalized emission spectra are presented at different doping potentials. The
10 shape of fluorescent emission remains unaffected upon doping up to $\eta = 0.15$ V and the
11 maximum stays at 594 nm, but it shifts to the blue when fluorescence is quenched at around
12 a half of its initial value. This hypsochromic displacement reaches 8 nm at $\eta = 0.32$ V, a point
13 where the emission from the polymer can be hardly detected. This behavior can be explained
14 in terms of the fall down of exciton lifetime at high level of electrochemical doping. In the
15 semiconducting state, the photogenerated excitons appear at different conjugated segments
16 of the polymer and they are able to migrate toward low energy chromophores, i.e. red sites
17 [28]. The generation of an increasing number of quenching centers promotes nonradiative
18 paths for de-excitation and at high level of doping, the probability of a given exciton to reach
19 a low energy site will be rather low. Under those conditions, the emission takes place
20 exclusively from non-aggregated polymer chains which are blue sites.

21
22 The overall electrochemical quenching of PL can be modeled using approaches like
23 those employed for solid-state fluorophores. When a photogenerated singlet exciton (S_1)
24 finds a quencher (p) an annihilation process like that described in Eq. 2 can occur [29]:
25



27
28 being k_q the annihilation polaron-exciton rate constant. This bimolecular process competes
29 with the monomolecular intrinsic de-excitation of excitons, described by a characteristic time
30 constant equal to the lifetime of the photogenerated excited state, τ_0 . Changes in the intensity
31
32
33
34
35
36
37
38
39
40
41
42
43
44
45
46
47
48
49
50
51
52
53
54
55
56
57
58
59
60
61
62
63
64
65

1
2
3
4 of emission in the presence of quenching sites generated by electrochemical doping can be
5
6 modeled to obtain Eq. 3, an expression equivalent to the Stern-Volmer equation (the detailed
7
8 derivation can be found in the supporting information in Section S2) [30]:
9

$$\frac{I_0}{I} = 1 + k_q \tau_0 [CD] \quad (3)$$

10
11
12
13
14
15
16
17 being I and I_0 the fluorescent intensity in the presence and in the absence of the quencher,
18
19 respectively, k_q the annihilation rate constant, τ_0 the characteristic lifetime for the
20
21 photogenerated excited state and $[CD]$ the quencher concentration (the injected charge
22
23 density).
24
25

26
27 Fig. 3.b shows the electrochemical Stern-Volmer plot determined experimentally for
28
29 MEH-PPV. At a low doping level, particularly below $CD= 3 \times 10^{18} \text{ cm}^{-3}$, the plot can be well
30
31 fitted to a straight line, as expected for a time-independent quenching rate in a purely
32
33 diffusion-controlled process (dynamic quenching). Such a linear trend reveals that a uniform
34
35 distribution of emitters and quenchers is preserved over the PL lifetime, as a result of fast
36
37 exciton diffusion [31]. Taking a fluorescence lifetime of $\tau_0= 140 \text{ ps}$ for MEH-PPV [32], the
38
39 quenching rate constant amounts to $k_q= 4.3 \times 10^{-9} \text{ cm}^3 \text{ s}^{-1}$. This polaron-exciton quenching rate
40
41 is nearly one order of magnitude lower than the exciton-exciton annihilation rate in this
42
43 polymer [32]. It is worth mentioning that the difference between annihilation constants
44
45 obtained from exciton-exciton and from electrochemical quenching of polyfluorene films
46
47 lays in the same order of magnitude [31].
48
49
50
51
52

53
54 At a charge density higher than $3 \times 10^{18} \text{ cm}^{-3}$ the positive deviation observed in Fig. 3 is
55
56 indicative of a combined quenching mechanism showing contributions of both diffusional
57
58 collision and direct exciton-polaron quenching by resonant energy transfer [31]. If the
59
60
61
62
63
64
65

1
2
3
4 treatment is limited to the linear zone of the Stern-Volmer plot, k_q follows the Smoluchowski
5
6 equation [33]:
7

$$k_q = 4\pi DR \quad (4)$$

8
9
10
11
12
13
14
15 in which D is the mutual diffusion coefficient of donor and acceptor species ($D_{exciton} +$
16 $D_{polaron}$) and R is the exciton-polaron annihilation critical distance. Eq. 4 allows determining
17
18 the exciton diffusion coefficient if the R parameter can be estimated. Gösele et al. [34]
19
20 proposed Eq. 5 to calculate donor-acceptor critical distances under experimental conditions
21
22 where the effect of exciton diffusion is significant:
23
24
25
26
27

$$R = 0.676 \left(\frac{R_0^6}{\tau_0 D} \right)^{1/4} \quad (5)$$

28
29
30
31
32
33
34
35
36
37 where R_0 is the transfer critical radius (or Förster critical radius) and the other symbols have
38
39 been defined above. The Förster critical radius can be derived from experimental data using
40
41 Eq. 6 [33,35]:
42
43

$$R_0(nm) = 0.0211 [Q_D \kappa^2 n^{-4} J]^{1/6} \quad (6)$$

44
45
46
47
48
49
50 here, Q_D is the emission quantum yield in the absence of energy transfer ($Q_D = 0.08$ [36]), κ^2
51
52 is the dipole orientation factor (0.476 for randomly oriented chromophores in solid state
53
54 [30]), n is the average refractive index of the medium in the wavelength range where spectral
55
56 overlap between donors and acceptors is significant, ($n = 1.97$ at 600 nm [37]). The spectral
57
58
59
60
61

1
2
3
4 overlap (J) can be evaluated from the emission and the absorbance spectra of doped MEH-
5
6 PPV to obtain a Förster radius from Eq. 6 of $R_0= 5.4$ nm and the exciton-polaron critical
7
8 distance is $R= 4.7$ nm, as derived from Eq. 5 (see section S3 in supporting information for
9
10 details). The mutual diffusion coefficient can be obtained from the experimental value of k_q
11
12 after the combination of Eqs. 4 and 5, resulting in $D= 7.2\times 10^{-4}$ cm² s⁻¹. To determine the
13
14 single diffusion coefficient of the exciton, D_{exciton} , it is essential to separate the contribution
15
16 to D coming from its associated quasiparticle (polaron). Since the polaron mobility in PPV
17
18 and related materials is typically within the range 10^{-11} to 10^{-5} cm² V⁻¹ s⁻¹ [38–40], at room
19
20 temperature D_{polaron} would be in the order of 10^{-13} to 10^{-7} cm² s⁻¹, as determined by the
21
22 Einstein relation, considering that in doped conjugated polymers the electric field inside the
23
24 material remains low thanks to charge compensation carried out by counterions [29]. Such a
25
26 small figure makes the contribution to D of this quasiparticle negligible. A comparison
27
28 between the obtained value and diffusion coefficients reported previously in the literature is
29
30 shown in Table 1. It is worth mentioning that the average bibliographic value matches exactly
31
32 the number derived from the analysis of the potential-dependent fluorescent emission carried
33
34 out in the present work.
35
36
37
38
39
40
41
42
43
44
45
46
47
48
49
50
51
52
53
54
55
56
57
58

59 **Table 1.** Bibliographic data reported for exciton diffusion coefficient in MEH-PPV
60
61

Determination Method	$D_{\text{exciton}} / \text{cm}^2 \text{ s}^{-1}$	Ref.
Steady-state PL quenching by dyes	7.2×10^{-4}	[5]
Transient PL quenching by exciton-exciton annihilation	3×10^{-3}	[32]
Polymer/fullerene bilayer photocell	5.8×10^{-4}	[41]
Transient PL quenching by photooxidized sites	2.0×10^{-4}	[42]
Transient PL quenching polymer/fullerene bilayer	11×10^{-4}	[43]
Electrochemical PL quenching	7.2×10^{-4}	this work

4. Conclusions

In this work, we checked the applicability of combined *in situ* electrochemical UV-vis and fluorescence spectroscopies as tools for the characterization of absorption and photoluminescent emission properties of neutral and electrochemically-doped conjugated polymer emitters. This is performed by employing MEH-PPV as a model luminescent polymer system.

The *p*-doping process of the polymer can be accurately and reversibly controlled by electrochemical methods and results in an accumulation of positively charged holes of polaronic nature, which behave as quenching sites for photoluminescence. At low *p*-doping level, the quenching process fits a Stern-Volmer quenching model, controlled by the diffusive motion of photogenerated excitons along the conjugated backbone. From the slope of the Stern-Volmer plot and the exciton-polaron critical distance derived from exciton emission and polaron absorption spectral overlap, an exciton diffusion coefficient of $7.2 \times 10^{-4} \text{ cm}^2 \cdot \text{s}^{-1}$ was estimated, in good agreement with the average value reported for MEH-PPV in the

1
2
3
4 literature. Electrochemical charge injection also brings about a progressive bleaching of the
5
6 polymer $\pi\pi^*$ transition and growth of the polaron absorption band, which is linear up to 0.01
7
8 charges per monomeric unit.
9

10
11 The successful analysis of the potential-dependent emission intensity of the
12
13 fluorescence quenching allows this methodology to be proposed as an alternative, fast and
14
15 powerful tool for the reliable measurement of exciton diffusion coefficients in conjugated
16
17 polymer films, and therefore it encourages its future application to the study of a wider range
18
19 of light-emitting systems.
20
21
22
23
24
25
26

27 **5. Acknowledgements**

28
29 This work was supported by Generalitat Valenciana (Conselleria de Educaci3n,
30
31 Investigaci3n, Cultura y Deporte) project PROMETEO/2018/087 and Spanish Ministerio de
32
33 Ciencia e Innovaci3n (project PID2019-105923RB-I00).
34
35
36
37
38
39
40
41
42
43
44

45 **6. References**

- 46
47
48 1. Tamai, Y.; Ohkita, H.; Bente, H.; Ito, S. Exciton Diffusion in Conjugated
49
50 Polymers: From Fundamental Understanding to Improvement in Photovoltaic
51
52 Conversion Efficiency. *J. Phys. Chem. Lett.* **2015**, *6*, 3417–3428.
53
54
55
56 2. Tang, S.; Sandstr3m, A.; Lundberg, P.; Lanz, T.; Larsen, C.; Van Reenen, S.;
57
58 Kemerink, M.; Edman, L. Design rules for light-emitting electrochemical cells
59
60
61
62
63
64
65

- 1
2
3
4 delivering bright luminance at 27.5 percent external quantum efficiency. *Nat.*
5
6
7 *Commun.* **2017**, *8*, 1190.
8
9
- 10 3. Menke, S.M.; Holmes, R.J. Exciton diffusion in organic photovoltaic cells. *Energy*
11
12 *Environ. Sci.* 2014, *7*, 499–512.
13
14
- 15 4. Vacar, D.; Maniloff, E.S.; McBranch, D.W. Charge-transfer range for
16
17 photoexcitations in conjugated polymer/fullerene bilayers and blends. *Phys. Rev. B -*
18
19 *Condens. Matter Mater. Phys.* **1997**, *56*, 4573–4577.
20
21
22
- 23 5. Bjorgaard, J.A.; Köse, M.E. Amplified quenching of conjugated polymer
24
25 nanoparticle photoluminescence for robust measurement of exciton diffusion length.
26
27 *J. Appl. Phys.* **2013**, *113*, 203707.
28
29
30
- 31 6. Wang, X.; Groff, L.C.; McNeill, J.D. Multiple energy transfer dynamics in blended
32
33 conjugated polymer nanoparticles. *J. Phys. Chem. C* **2014**, *118*, 25731–25739.
34
35
36
- 37 7. Furukawa, Y. Electronic absorption and vibrational spectroscopies of conjugated
38
39 conducting polymers. *J. Phys. Chem.* **1996**, *100*, 15644–15653.
40
41
42
- 43 8. Montilla, F.; Ruseckas, A.; Samuel, I.D.W. Absorption cross-sections of hole
44
45 polarons in glassy and beta-phase polyfluorene. *Chem. Phys. Lett.* **2013**, *585*, 133–
46
47 137.
48
49
- 50 9. Scholes, D.T.; Yee, P.Y.; Lindemuth, J.R.; Kang, H.; Onorato, J.; Ghosh, R.;
51
52 Luscombe, C.K.; Spano, F.C.; Tolbert, S.H.; Schwartz, B.J. The Effects of
53
54 Crystallinity on Charge Transport and the Structure of Sequentially Processed
55
56 F4TCNQ-Doped Conjugated Polymer Films. *Adv. Funct. Mater.* **2017**, *27*, 1702654.
57
58
59
60
61
62
63
64
65

- 1
2
3
4 10. Al-Kutubi, H.; Zafarani, H.R.; Rassaei, L.; Mathwig, K. Electrofluorochromic
5 systems: Molecules and materials exhibiting redox-switchable fluorescence. *Eur.*
6 *Polym. J.* 2016, 83, 478–498.
7
8
9
10
11
12 11. Audebert, P.; Miomandre, F. Electrofluorochromism: from molecular systems to set-
13 up and display. *Chem. Sci.* **2013**, 4, 575–584.
14
15
16
17 12. Zhai, Y.; Zhu, Z.; Zhou, S.; Zhu, C.; Dong, S. Recent advances in
18 spectroelectrochemistry. *Nanoscale* 2018, 10, 3089–3111.
19
20
21
22
23 13. Kim, S.; You, Y. Highly Reversible Electrofluorochromism from Electrochemically
24 Decoupled but Electronically Coupled Molecular Dyads. *Adv. Opt. Mater.* **2019**,
25 1900201.
26
27
28
29
30
31 14. Corrente, G.A.; Beneduci, A. Overview on the Recent Progress on
32 Electrofluorochromic Materials and Devices: A Critical Synopsis. *Adv. Opt. Mater.*
33 **2020**, 8.
34
35
36
37
38
39 15. Čížková, M.; Cattiaux, L.; Mallet, J.M.; Labbé, E.; Buriez, O. Electrochemical
40 switching fluorescence emission in rhodamine derivatives. *Electrochim. Acta* **2018**,
41 260, 589–597.
42
43
44
45
46
47 16. Yen, H.J.; Liou, G.S. Design and preparation of triphenylamine-based polymeric
48 materials towards emergent optoelectronic applications. *Prog. Polym. Sci.* 2019, 89,
49 250–287.
50
51
52
53
54
55 17. Seo, S.; Shin, H.; Park, C.; Lim, H.; Kim, E. Electrofluorescence switching of
56 fluorescent polymer film. *Macromol. Res.* 2013, 21, 284–289.
57
58
59
60
61
62
63
64
65

- 1
2
3
4 18. Ding, G.; Zhou, H.; Xu, J.; Lu, X. Electrofluorochromic detection of cyanide anions
5 using a benzothiadiazole-containing conjugated copolymer. *Chem. Commun.* **2014**,
6
7 50, 655–657.
8
9
- 10
11
12 19. Beaujuge, P.M.; Fréchet, J.M.J. Molecular design and ordering effects in π -
13 functional materials for transistor and solar cell applications. *J. Am. Chem. Soc.*
14
15 **2011**, *133*, 20009–20029.
16
17
18
19
- 20 20. Schwartz, B.J. Conjugated polymers as molecular materials: how chain conformation
21 and film morphology influence energy transfer and interchain interactions. *Annu.*
22
23 *Rev. Phys. Chem.* **2003**, *54*, 141–72.
24
25
26
27
- 28 21. Montilla, F.; Pastor, I.; Mateo, C.R.; Morallon, E.; Mallavia, R.; Morallón, E.;
29 Mallavia, R. Charge transport in luminescent polymers studied by in situ
30 fluorescence spectroscopy. *J. Phys. Chem. B* **2006**, *110*, 5914–5919.
31
32
33
34
35
- 36 22. Santos, L.F.; Faria, R.C.; Gaffo, L.; Carvalho, L.M.; Faria, R.M.; Gonçalves, D.
37 Optical, electrochemical and electrogravimetric behavior of poly(1-methoxy-4-(2-
38 ethyl-hexyloxy)-p-phenylene vinylene) (MEH-PPV) films. *Electrochim. Acta* **2007**,
39
40 52, 4299–4304.
41
42
43
44
45
- 46 23. Cardona, C.M.; Li, W.; Kaifer, A.E.; Stockdale, D.; Bazan, G.C. Electrochemical
47 considerations for determining absolute frontier orbital energy levels of conjugated
48 polymers for solar cell applications. *Adv. Mater.* **2011**, *23*, 2367–2371.
49
50
51
52
53
- 54 24. Holt, A.L.; Leger, J.M.; Carter, S.A. Electrochemical and optical characterization of
55 p- and n-doped poly[2-methoxy-5-(2-ethylhexyloxy)-1,4-phenylenevinylene]. *J.*
56
57 *Chem. Phys.* **2005**, *123*.
58
59
60
61
62
63
64
65

- 1
2
3
4 25. Fernandas, M.R.; Garcia, J.R.; Schultz, M.S.; Nart, F.C. Polaron and bipolaron
5
6 transitions in doped poly(p-phenylene vinylene) films. *Thin Solid Films* **2005**, *474*,
7
8 279–284.
9
- 10
11 26. Candeias, L.P.; Grozema, F.C.; Padmanaban, G.; Ramakrishnan, S.; Siebbeles,
12
13 L.D.A.; Warman, J.M. Positive charge carriers on isolated chains of MEH-PPV with
14
15 broken conjugation: Optical absorption and mobility. *J. Phys. Chem. B* **2003**, *107*,
16
17 1554–1558.
18
19
20
21
22 27. Ho, P.K.H.; Thomas, D.S.; Friend, R.H.; Tessler, N. All-polymer optoelectronic
23
24 devices. *Science (80-.)*. **1999**, *285*, 233–236.
25
26
27
28 28. Martini, I.B.; Smith, A.D.; Schwartz, B.J. Exciton-exciton annihilation and the
29
30 production of interchain species in conjugated polymer films: Comparing the
31
32 ultrafast stimulated emission and photoluminescence dynamics of MEH-PPV. *Phys.*
33
34 *Rev. B - Condens. Matter Mater. Phys.* **2004**, *69*, 035204.
35
36
37
38 29. van Reenen, S.; Vitorino, M. V; Meskers, S.C.J.; Janssen, R.A.J.; Kemerink, M.
39
40 Photoluminescence quenching in films of conjugated polymers by electrochemical
41
42 doping. *Phys. Rev. B* **2014**, *89*.
43
44
45
46 30. Valeur, B. *Molecular Fluorescence. Principles and Applications*; 1st ed.; Wiley-
47
48 VCH Verlag GmbH, 2001; ISBN 3-527-29919-X.
49
50
51
52 31. Montilla, F.; Ruseckas, A.; Samuel, I.D.W. Exciton-Polaron Interactions in
53
54 Polyfluorene Films with β -Phase. *J. Phys. Chem. C* **2018**, *122*.
55
56
57
58 32. Lewis, A.J.; Ruseckas, A.; Gaudin, O.P.M.; Webster, G.R.; Burn, P.L.; Samuel,
59
60 I.D.W. Singlet exciton diffusion in MEH-PPV films studied by exciton-exciton
61
62
63
64
65

- 1
2
3
4 annihilation. *Org. Electron.* **2006**, *7*, 452–456.
5
6
7
8 33. Lakowicz, J.R. *Principles of Fluorescence Spectroscopy*; Plenum Press: New York,
9
10 2013; ISBN 0306412853.
11
12
13 34. Gosele, U.; Hauser, M.; Klein, U.K.A.; Frey, R. Diffusion and Long-Range Energy-
14
15 Transfer. *Chem. Phys. Lett.* **1975**, *34*, 519–522.
16
17
18 35. Rolinski, O.J.; Birch, D.J.S. Determination of acceptor distribution from
19
20
21
22
23
24
25
26
27
28
29
30
31
32
33
34
35
36
37
38
39
40
41
42
43
44
45
46
47
48
49
50
51
52
53
54
55
56
57
58
59
60
61
62
63
64
65
- annihilation. *Org. Electron.* **2006**, *7*, 452–456.
33. Lakowicz, J.R. *Principles of Fluorescence Spectroscopy*; Plenum Press: New York, 2013; ISBN 0306412853.
34. Gosele, U.; Hauser, M.; Klein, U.K.A.; Frey, R. Diffusion and Long-Range Energy-Transfer. *Chem. Phys. Lett.* **1975**, *34*, 519–522.
35. Rolinski, O.J.; Birch, D.J.S. Determination of acceptor distribution from fluorescence resonance energy transfer: Theory and simulation. *J. Chem. Phys.* **2000**, *112*, 8923–8933.
36. Marchioni, F.; Chiechi, R.; Patil, S.; Wudl, F.; Chen, Y.; Shinar, J. Absolute photoluminescence quantum yield enhancement of poly(2-methoxy 5-[2'-ethylhexyloxy]-p-phenylenevinylene). *Appl. Phys. Lett.* **2006**, *89*, 061101.
37. Tammer, M.; Monkman, A.P. Measurement of the anisotropic refractive indices of spin cast thin poly(2-methoxy-5-(2'-ethyl-hexyloxy)-p-phenyl-enevinylene) (MEH-PPV) films. *Adv. Mater.* **2002**, *14*, 210–212.
38. Tuladhar, S.M.; Poplavskyy, D.; Choulis, S.A.; Durrant, J.R.; Bradley, D.D.C.; Nelson, J. Ambipolar Charge Transport in Films of Methanofullerene and Poly(phenylenevinylene)/Methanofullerene Blends. *Adv. Funct. Mater.* **2005**, *15*, 1171–1182.
39. Blom, P.W.M.; de Jong, M.J.M.; van Munster, M.G. Electric-field and temperature dependence of the hole mobility in poly(p-phenylene vinylene). *Phys. Rev. B* **1997**, *55*, R656–R659.

1
2
3
4
5
6
7
8
9
10
11
12
13
14
15
16
17
18
19
20
21
22
23
24
25
26
27
28
29
30
31
32
33
34
35
36
37
38
39
40
41
42
43
44
45
46
47
48
49
50
51
52
53
54
55
56
57
58
59
60
61
62
63
64
65

40. Jiang, X.; Harima, Y.; Zhu, L.; Kunugi, Y.; Yamashita, K.; Sakamoto, M.; Sato, M. Mobilities of charge carriers hopping between π -conjugated polymer chains. *J. Mater. Chem.* **2001**, *11*, 3043–3048.
41. Halls, J.J.M.; Pichler, K.; Friend, R.H.; Moratti, S.C.; Holmes, A.B. Exciton diffusion and dissociation in a poly(p-phenylenevinylene)/C60 heterojunction photovoltaic cell. *Appl. Phys. Lett.* **1996**, *68*, 3120–3122.
42. Yan, M.; Rothberg, L.J.; Papadimitrakopoulos, F.; Galvin, M.E.; Miller, T.M. Defect quenching of conjugated polymer luminescence. *Phys. Rev. Lett.* **1994**, *73*, 744–747.
43. Markov, D.E.; Tanase, C.; Blom, P.W.M.; Wildeman, J. Simultaneous enhancement of charge transport and exciton diffusion in poly(p-phenylene vinylene) derivatives. *Phys. Rev. B - Condens. Matter Mater. Phys.* **2005**, *72*, 045217.